

# Instabilities in a running superfluid and stripe supersolid

Jinwu Ye

<sup>1</sup> Institute for Theoretical Sciences, Westlake University, Hangzhou, 310024, Zhejiang, China

<sup>2</sup> Department of Physics and Astronomy, Mississippi State University, MS, 39762, USA

(Dated: July 15, 2022)

The possible instabilities in a running superfluid has been a long-time historical problem since first studied by L. P. Landau. By constructing effective actions in terms of suitable order parameters, we revisit this outstanding open problem. We find that if the instability is driven by the SF Goldstone mode near  $k = 0$ , then there is a quantum Lifshitz transition from the SF to a Boosted SF (BSF) with the dynamic exponent ( $z_x = 3/2, z_y = 3$ ) subject to logarithmic corrections from a marginally irrelevant cubic term. This case may happen to exciton superfluids in bilayer quantum Hall systems or electron-hole bilayer systems, especially in weakly interacting Bose gas in cold atom systems. If the instability is driven by the roton mode near a finite momentum  $k = k_0$ , then there is a SF to a stripe supersolid transition with the dynamic exponent  $z = 1$  which is in the same universality class as the  $z = 1$  boosted Mott-SF transition studied previously in a different context. This case may apply to Helium 4 and also cold atom BECs where the rotons in the SF phase plays an important role. Driving a SF sufficiently fast may become an effective way to create a SS which is a long time sought novel state of matter.

**1. Introduction:** It is well known that many systems become a superfluid at sufficiently low temperatures [1]. He4 or He3 is the oldest strongly interacting bosonic or fermionic systems which become a SF below  $T_c \sim 2.17K$  and  $T_c \sim 1mK$  respectively. Then weakly interacting superfluid systems were created in bosonic [2] and fermionic [3] charge neutral atoms at even lower temperature  $\sim nK$ . There are also some experimental evidences to suggest exciton superfluid of electrons and holes may have been realized in the bilayer quantum Hall systems at the total filling factor  $\nu_T = 1$  [4, 5] or electron-hole bilayer with sufficiently long lifetime [6]. In a quantum magnet subject to a Zeeman field, the  $U(1)_s$  spin rotation symmetry around the Zeeman field resembles the global  $U(1)$  symmetry in the interacting bosons [7], the magnon condensations leading to some magnetic ordered phases can be mapped to the boson condensations leading to the SF. Recently, this mapping was also found in quantum magnets with spin-orbital couplings (SOC) in a longitudinal Zeeman field [8].

The physics of driving an object inside a superfluid (SF) or driving the SF itself has a long history [10–13]. It may be necessary to distinguish the two different, but related cases: (1) Controlling the moving object: An impurity moving in a superfluid. It was discussed in [10, 13] and more recently in [14]. If an object moves in a superfluid at  $T = 0$  with a velocity below the critical velocity  $v < v_c^0$ , there is no viscosity. However, when  $v > v_c^0$ , a viscosity arises due to the emission of elementary excitations such as vortex rings [11, 12]. (2) Controlling the superfluid: The SF is flowing with a finite velocity  $v$ . It was also discussed in [10, 13] and more recently in [15]. The flow of a SF with  $v > v_c^{SF}$  may not destroy SF, but the order parameter may develop small additional components around a roton minimum, therefore reduce the superfluid density. However, when increasing  $v$  further, the fate of SF is still not known yet. The first class is

an non-equilibrium driven system which was experimentally investigated in cold atom BEC, by pulling an optical lattice[9], the second is an equilibrium steady one. In this manuscript, we focus on the second class from effective action approach in either phase or dual density representation whichever is suitable. We will also establish some intrinsic connections between this class and a seemingly unrelated problem: the fate of liquid Helium under the increasing pressure.

The global Pressure-Temperature (T-P) phase diagram of the Helium-4 is shown in Fig.1a ([13]). The elementary excitations in the Helium-4 contains the SF phonon part near  $k \sim 0$  and the roton part near  $k = k_0$  (Fig.1b). In this well known T-P diagram, there maybe a room to host a possible tantalizing supersolid phase which has both the SF order and the solid order [16]. In 2005, by using torsional oscillator measurement, Chan's group [17] observed a marked  $1 \sim 2\%$  non-classical rotational inertial (NCRI) of the solid 4He at  $\sim 0.2K$ , both when embedded in Vycor glass and in bulk Helium 4. The authors suggested that the NCRI may suggest the supersolid state of 4He. These experimental results inspired extensive theoretical [18, 19] and experimental interests to examine the very intriguing supersolid phase of 4He. However, a later refined experiment [20] excludes the putative SS in Fig.1a. Despite its absence in the He4 system, the SS phase is an interesting phase on its own. It was shown to exist in a lattice system [21–27]. Of course, the SS in a lattice system is quite different than that in a continuum system [19]. In this manuscript, we will show that the SS may also exist in Helium 4 under a sufficiently large flow, namely the second class of problem in the last paragraph.

In this work, we develop an systematic and unified effective action approach in both the phase and its dual magnitude representation to study all the possible instabilities and quantum phase transitions (QPT) by driving

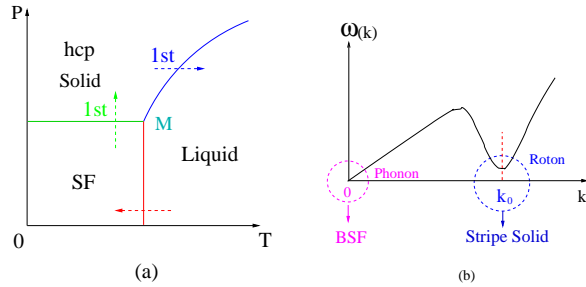


FIG. 1. (a) The pressure  $P$  and temperature  $T$   $\text{He4}$  phase diagram with  $T_c \sim 2.13\text{K}$  and  $P_c \sim 120\text{bar}$ . The liquid to SF transition is in a classical 3d XY class for any pressure  $0 < P < P_c$  which is also exactly marginal. The SF to solid transition is a first order quantum Lifshitz transition triggered by the lowering of roton surface tuned by the pressure. The liquid to solid transition is a first order classical Lifshitz transition driven by the peak in the density-density correlation tuned also by the pressure. (b) The elementary excitation in the SF phase. The roton surface is spherically symmetric with the roton gap  $\Delta/k_B \sim 10\text{K}$  and  $k_0 \sim 2\text{\AA}^{-1}$ .

a SF beyond some critical velocities. If the instability is due to the SF Goldstone mode near  $k = 0$ , then there is a quantum Lifshitz transition from the SF to a boosted SF (BSF) with the dynamic exponent ( $z_x = 3/2, z_y = 3$ ) and a marginally irrelevant cubic term. We work out the excitation spectrum in both phases, perform the renormalization group analysis and evaluate the scaling functions at a finite  $T$  near the QPT. This scenario may apply to the exciton SF in BLQH [4, 5] and EBL [6] where the magneto-roton exists only at a very high energy, especially in cold atom BEC systems with low critical velocities [2, 3]. If the instability is due to the roton mode near  $k = k_0$ , then there is a SF to a stripe supersolid (SSS) transition with the dynamic exponent  $z = 1$  which is in the same universality class of the boosted Mott-SF transition studied in [8, 29] with an emergent C- symmetry. We also analyze the symmetry breaking and the excitation spectrum in the SSS phase. Then as the boost increases further, there is a QPT from the SSS to the stripe solid with  $z = 2$ . From the general symmetry breaking principle, we argue that the resulting stripe solid may also have vacancies whose BEC may lead to the SSS. We show that the driving is a new and effective mechanism to generate a supersolid which is a long time elusive goal in low temperature physics and can be realized not only in  $\text{He4}$ , but also in various cold atom systems with long-range dipole-dipole interactions, spin-orbit couplings or dressed by Rydberg atoms.

## 2. Co-moving frame and the lab frame in a running SF

In the co-moving frame with the SF, the SF is static. In terms of the SF order parameter  $\psi = \sqrt{\rho_0 + \delta\rho}e^{i\phi}$ , one

just takes the effective action inside the SF phase [28]:

$$\mathcal{L}_{M:\text{SF}}[\delta\rho, \phi] = i\delta\rho\partial_\tau\phi + \rho_0[v_x^2(\partial_x\phi)^2 + v_y^2(\partial_y\phi)^2] + u(\delta\rho)^2 + w\rho_0(\partial_y\phi)^3 + \dots \quad (1)$$

where, in addition to phase-magnitude conjugation  $i\delta\rho\partial_\tau\phi$ , the last cubic term also breaks the Charge conjugation (C-) symmetry  $\phi \rightarrow -\phi$  in the  $(\delta\rho, \phi)$  representation.

Now one gets to the lab frame just by performing a Galileo transformation (GT) [8, 29]  $\partial_\tau \rightarrow \partial_\tau - ic\partial_y$  (we drop the 't'):

$$\mathcal{L}_{L:\text{SF}}[\delta\rho, \phi] = i\delta\rho\partial_\tau\phi + \rho_0[v_x^2(\partial_x\phi)^2 + v_y^2(\partial_y\phi)^2] + u(\delta\rho)^2 + w\rho_0(\partial_y\phi)^3 + c\delta\rho\partial_y\phi \quad (2)$$

where the boost velocity was pinned to be  $\vec{c} = \vec{Q}/m$ .

The order parameter in the lab frame becomes

$$\psi_{SF} = \sqrt{\rho_0 + \delta\rho}e^{i(\vec{Q}\cdot\vec{x} + \phi)} \quad (3)$$

which carries a SF flow in the lab frame.

In the following, we will study the possible instability when the flow is beyond a critical one from both phase representation and its dual magnitude representation in the lab frame. The C- symmetry case was addressed in [8] in a completely different context: a quantum magnet with SOC in a longitudinal Zeeman field. The C- symmetry only exists in a lattice system at integer fillings [8, 29, 30]. However, there is no C- symmetry in all the continuous SF systems mentioned in the introduction. It is the absence of the C- symmetry which leads to the new QPTs in all the following sections [31].

### 3. The quantum Lifshitz transition from the SF to the BSF driven by the instability in the Goldstone mode

Taking  $\vec{c} = \vec{Q}/m$  as an independent tuning parameter, we will study the putative SF to the BSF transition tuned by this boost.

After integrating out the magnitude fluctuations in Eq.2, the quantum phase fluctuations are described by:

$$\mathcal{L}_{L:\text{SF}}[\phi] = \frac{1}{2u}(\partial_\tau\phi - ic\partial_x\phi)^2 + \rho_0[v_x^2(\partial_x\phi)^2 + v_y^2(\partial_y\phi)^2] + w\rho_0(\partial_y\phi)^3 \quad (4)$$

Now we study how the SF evolves as one increases  $\vec{Q}$ . The mean-field state can be written as  $\phi = \phi_0 + k_0y$ . Substituting it to the effective action Eq.4 leads to:

$$\mathcal{S}_0 \propto (2U\rho_0v_y^2 - c^2)k_0^2 + 2wU\rho_0k_0^3 \quad (5)$$

At a low boost  $c^2 < 2U\rho_0v_y^2$ ,  $k_0 = 0$  is in the SF phase. Its spectrum is given by:

$$\omega = \sqrt{2w\rho_0(v_x^2k_x^2 + v_y^2k_y^2)} - ck_y \quad (6)$$

At the critical boost between the SF and the boosted SF

$$c^2 = 2U\rho_0v_y^2 \quad (7)$$

which gives the phase boundary in Fig.2a.

At a high boost  $c^2 > 2U\rho_0v_y^2$

$$k_0 = \frac{c^2 - 2U\rho_0v_y^2}{3wU\rho_0} \quad (8)$$

where  $w \propto c$ , so its sign is completely determined by the driving. So the BSF phase has an additional modulation  $k_0$  along the  $y$ -axis on top of Eq.3:

$$\psi_{BSF} = \sqrt{\rho_0 + \delta\rho} e^{i[(\vec{Q} + \vec{k}_0) \cdot \vec{x} + \phi]} \quad (9)$$

Inside the BSF phase, the quantum phase fluctuations can be written as  $\phi \rightarrow \phi_0 + k_0y + \phi$ . Expanding the action upto the second order in the phase fluctuations leads to

$$\begin{aligned} \mathcal{L}_{BSF} = & (\partial_\tau\phi - ic\partial_y\phi)^2 + 2U\rho_0v_x^2(\partial_x\phi)^2 \\ & + (2c^2 - 2U\rho_0v_y^2)(\partial_y\phi)^2 \\ & + 2wU\rho_0(\partial_y\phi)^3 + b(\partial_y\phi)^4 + \dots \end{aligned} \quad (10)$$

which leads to the gapless Goldstone mode inside the BSF phase:

$$\omega_{\mathbf{k}} = \sqrt{2U\rho_0v_x^2k_x^2 + (2c^2 - 2U\rho_0v_y^2)k_y^2 - ck_y} \quad (11)$$

where one can see  $2c^2 - 2U\rho_0v_y^2 = c^2 + (c^2 - 2U\rho_0v_y^2) > c^2$  when  $c^2 > 2U\rho_0v_y^2$ , thus the  $\omega_{\mathbf{k}}$  is stable in BSF phase.

It is instructive to expand the first kinetic term in Eq.4 as:

$$\begin{aligned} 2U\mathcal{L} = & Z(\partial_\tau\phi)^2 - 2ic\partial_\tau\phi\partial_y\phi + 2U\rho_0v_x^2(\partial_x\phi)^2 + \gamma(\partial_y\phi)^2 \\ & + a(\partial_y^2\phi)^2 + 2wU\rho_0(\partial_y\phi)^3 + b(\partial_y\phi)^4 \end{aligned} \quad (12)$$

where  $Z$  is introduced to keep track of the renormalization of  $(\partial_\tau\phi)^2$ ,  $\gamma = 2U\rho_0v_y^2 - c^2$  is the tuning parameter.

The scaling  $\omega \sim k_y^3, k_x \sim k_y^2$  leads to the exotic dynamic exponents ( $z_x = 3/2, z_y = 3$ ). Then one can get the scaling dimension of  $[\gamma] = 2$  which is relevant, as expected, to tune the transition, but  $[Z] = [b] - 2 < 0$ , so are two leading irrelevant operators which determine the finite  $T$  behaviours and corrections to the leading scalings. However  $[w] = 0$  is marginal. The standard field theory one-loop RG finds:

$$\frac{dw}{dl} = \epsilon w - Aw^2 \quad (13)$$

where  $\epsilon = 2 - d$  and  $A = 1/v_x^2a > 0$ . So it is marginally irrelevant. Setting  $Z = w = 0$  in Eq.12 leads to the Gaussian fixed point action at the QCP where  $\gamma = 0$ , subject to the Logarithmic correction due to the marginally irrelevant  $w$  term. Again it is the crossing metric  $g_{\tau,y} = g_{y,\tau} = -ic$  in Eq.12 which dictates the quantum dynamic

scaling near the QCP. It is a direct reflection of the new emergent space-time near the  $z = (3/2, 3)$  QPT. Note that here the QPT is a quantum Lifshitz one tuned by  $[\gamma] = 2$ , so despite the cubic term  $[w] = 0$ , it could still be a 2nd -order transition in Fig.2a, in contrast to the conventional QPT where a cubic term drives a first order one.

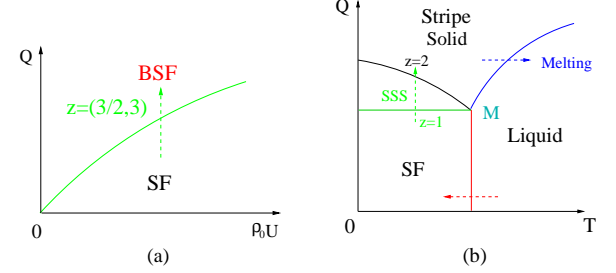


FIG. 2. The instabilities of driving a SF. In the absence of a roton, the instability happens near the origin ( the phonon mode ), it leads to a BSF phase in (a). If there exists of a roton such as in He4, the instability at  $k = 0$  will always be pre-empted by that near the roton. Then the instability near the roton minimum leads to a stripe supersolid (SSS) phase in (b). The QPT from the SF to the SSS is in the same universality class as that from the boosted Mott to the SF with  $z = 1$  [8, 29]. There is also a QPT from the SSS to the stripe solid with  $z = 2$ . The finite temperature melting transition from the stripe solid to the normal liquid is also in the 3d XY universality class. The vacancies BEC in the stripe solid leads to the SSS intervening between the SF and the stripe solid. The order parameters in all the 4 phases are: Normal liquid  $\langle\psi_0\rangle = 0, \langle\psi_G\rangle = 0$ , SF  $\langle\psi_0\rangle \neq 0, \langle\psi_G\rangle = 0$ , Stripe solid  $\langle\psi_0\rangle = 0, \langle\psi_G\rangle \neq 0$ , SSS  $\langle\psi_0\rangle \neq 0, \langle\psi_G\rangle \neq 0$ .

Now we evaluate the conserved currents in both SF and BSF phase. The  $U(1)$  symmetry in the normal phase transpire as  $\phi \rightarrow \phi + a$  for any shift  $a$  inside the  $U(1)$  symmetry broken SF phase, so the Noether current can be derived from Eq.4 as:

$$J_\tau = 2(\partial_\tau\phi - ic\partial_y\phi)$$

$$J_x = 4u\rho_0v_x^2\partial_x\phi$$

$$\tilde{J}_y = J_y - icJ_\tau = 2u\rho_0[2v_y^2(\partial_y\phi) + 3w(\partial_y\phi)^2] - icJ_\tau \quad (14)$$

In the SF phase,  $\phi = \phi_0$ , then  $(J_\tau, J_x, \tilde{J}_y) = (0, 0, 0)$  and  $(J_\tau, J_x, J_y) = (0, 0, 0)$  also. In the BSF phase,  $\phi = \phi_0 + k_0y$  where  $k_0$  is given by Eq.8, then  $(J_\tau, J_x, \tilde{J}_y) = (-i2ck_0, 0, 0)$ , but  $(J_\tau, J_x, J_y) = (-i2ck_0, 0, 2c^2k_0)$ . So the conserved currents  $(J_\tau, J_x, J_y)$  can still be used to distinguish the BSF from the SF phase.

However, if there exists roton shown in Fig.1c, then this SF to BSF transition will be preempted by the the SF to a solid transition triggered by the roton touchdown as shown in the following sections.

#### 4. The SF to the SF density wave transition driven by the instability in the roton mode

In Helium 4, due to the long-range Wan der-Waals interaction, the density-density interaction  $V_d(q)$  develops

a roton minimum which drives the transition from the SF to a solid [19]. Now the density-density interaction  $U$  becomes long-ranged in Helium 4, so we adopt the notation in [28] as  $U = V_d(k) = a - bk^2 + \alpha k^4$  which can be written as  $V_d(k) = r + \alpha(k^2 - k_0^2)^2$  near the roton minimum (Fig.1c). We also consider the isotropic case  $v_x^2 = v_y^2$ , then  $\rho_s = \rho_0 v_x^2 = \rho_0 v_y^2$  is the superfluid density,  $\kappa^{-1} = \lim_{k \rightarrow 0} V_d(k) = a$  is the compressibility and  $v^2(k) = \rho_s V_d(k)$ .

From Eq.3, one can see that the density stays the same in both the lab frame and the co-moving frame. The dynamic structure factor is:

$$S_n^>(\vec{k}, \omega) = S_n(\vec{k})\delta(\omega - \epsilon_+(\vec{k})), \quad S_n(\vec{k}) = \frac{\pi\rho_s k}{2v(k)} \quad (15)$$

where  $\epsilon_+(\vec{k}) = v(k)k + ck_x$  is the quasi-particle excitation energy.

It is easy to see that a generalized Feynman relation still holds under the driving:

$$\epsilon_+(\vec{k}) = \frac{\int_0^\infty d\omega \omega S_n^>(\vec{k}, \omega)}{\int_0^\infty d\omega S_n^>(\vec{k}, \omega)} \quad (16)$$

A similar relation for the quasi-hole excitation energy  $\epsilon_-(\vec{k}) = v(k)k - ck_x$  can be derived by replacing  $S_n^>(\vec{k}, \omega)$  by  $S_n^<(\vec{k}, \omega)$ .

After integrating out the phase fluctuations in Eq.2, the quantum magnitude fluctuations can be used to describe such a transition under a driving:

$$\begin{aligned} \mathcal{L}[\delta\rho] = & \frac{1}{2}\delta\rho(-k, -\omega)\left[\frac{\omega^2 + i2c\omega k_x}{\rho_s k^2} + (r - \frac{c^2 k_x^2}{\rho_s k^2})\right. \\ & \left. + \alpha(k^2 - k_0^2)^2\right]\delta\rho(k, \omega) - w(\delta\rho)^3 + u(\delta\rho)^4 + \dots \end{aligned} \quad (17)$$

where  $r$  is the roton gap near  $k = k_0$ . Again the cubic term in the density-density channel need to be included at the very beginning.

The  $U$  term nails down the momentum  $k$  to be in the roton ring  $k = k_0$ , the boost term pins it to be in the  $k_x$  axis  $k_x = \pm k_0$ . So the boost term just introduce an easy-axis to the isotropic roton mode. So the resulting solid has only two shortest reciprocal lattice vectors  $\vec{G} = \pm k_0 \hat{x}$ :

$$\begin{aligned} n = & n_0 + (\psi_G e^{ik_0 x} + \psi_G^* e^{-ik_0 x}) \\ = & n_0 + 2|\psi_G| \cos(k_0 x + \alpha) \end{aligned} \quad (18)$$

where  $\psi_G$  is the complex order parameter. Its phase  $\alpha$  is the gapless phonon mode due to the translational symmetry breaking. It is the stripe solid phase. In fact, as shown in [34], even without such an easy axis term which explicitly breaks the rotational symmetry, a strip solid phase is most likely to be the ground state lattice structure due to the spontaneously lattice symmetry breaking. In the presence of such an easy axis term, the stripe solid is the ground state.

Then writing  $k_x = \pm k_0 + q_x, k_y = q_y$  and expanding up to the quartic term, we obtain:

$$\begin{aligned} \mathcal{L}[\delta\rho] = & \frac{1}{2}\delta\rho(-k, -\omega)\left[\frac{\omega^2 + i2c\omega q_x}{\rho_s k_0^2} + 4\alpha k_0^2 q_x^2 + \frac{c^2}{\rho_s k_0^2} q_y^2\right. \\ & \left. + \tilde{r}\right]\delta\rho(k, \omega) - w(\delta\rho)^3 + u(\delta\rho)^4 + \dots \end{aligned} \quad (19)$$

where  $\tilde{r} = r - c^2/\rho_s$  is the boosted roton gap and  $k_x = \pm k_0 + q_x, k_y = q_y$  need to be summed around both regimes near  $\pm k_0$ . Using the decomposition Eq.18, one obtain the effective action describing the SF to the stripe solid transition [36]:

$$\begin{aligned} \mathcal{L}[\psi_G] = & \frac{1}{2}\psi_G^*(k, \omega)\left[\frac{\omega^2 + i2c\omega q_x}{\rho_s k_0^2} + 4\alpha k_0^2 q_x^2 + \frac{c^2}{\rho_s k_0^2} q_y^2\right. \\ & \left. + \tilde{r}\right]\psi_G(k, \omega) + u|\psi_G(k, \omega)|^4 + \dots \end{aligned} \quad (20)$$

where due to the stripe structure, the cubic term plays no role. In fact as shown in [34], the cubic term play an important role only in a triangular lattice where the three shortest reciprocal lattice vectors form a closed triangle.

Substituting Eq.18 into Eq.3, we get the corresponding order parameter:

$$\psi_{SSDW} = \sqrt{\rho_0} e^{i(\vec{Q} \cdot \vec{x} + \phi)} [1 + |\psi_G| \cos(k_0 x + \alpha)/\rho_0] \quad (21)$$

which establishes the relation between the physical quantity  $\psi_{SSDW}$  and the order parameter  $\psi_G$  in the effective action Eq.20. The translational symmetry  $x \rightarrow x + a$  in Eq.18 translates into the  $U(1)_T$  symmetry of  $\psi_G \rightarrow \psi_G e^{ik_0 a}$  where its phase  $\theta = k_0 a$  is any continuous real number [35]. The  $U(1)_T$  symmetry breaking leads to the Goldstone mode which is the phonon mode  $\alpha$  in Eq.18 due to the translational symmetry breaking to the SSDW phase. It breaks the  $U(1)_I \times U(1)_T$  symmetry leading to the two Goldstone modes  $\phi, \alpha$  which are the superfluid and lattice Goldstone mode respectively.

Eq.20 is nothing but in the same universality class of QPT from the boosted Mott to SF along the Path-I in Fig.3a in [29]. So it has the dynamic exponent  $z_x = z_y = 1$ , the boost  $c$  is exactly marginal. Setting  $\tilde{r} = \Delta - c^2/\rho_s = 0$  leads to the critical velocity:

$$c^2 = \rho_s \Delta \quad (22)$$

which gives the SF to the SSDW phase boundary in Fig.2b. When  $\tilde{r} > 0, \langle \psi_G \rangle = 0$ , it is in the SF phase. When  $\tilde{r} < 0, \langle \psi_G \rangle \neq 0$ , it is in the Stripe SF density wave (SFDW) phase. Despite the original action Eq.2 has no C-symmetry, it has an emergent C-symmetry in the effective action Eq.20.

The main differences between the BSF in Eq.9 and the SSDW in Eq.21 is that in the former, it is completely a phase driven QPT, so there is only one wavevector component  $\vec{Q} + \vec{k}_0$ , it has only one gapless Goldstone mode  $\phi$ , while in the latter, it is magnitude driven QPT, so there are three wavevector components  $\vec{Q}$  and  $\vec{Q} \pm \vec{k}_0$  which

leads to the magnitude modulation in Eq.21. it has two gapless Goldstone modes  $\phi$  and  $\alpha$ .

5. *Crossover from the SSDW to the stripe supersolid.* Eq.21 holds near the SF to the SSDW transition. As one increases the boost further, the superfluid density  $\rho_s$  starts to decrease as the normal solid component  $|\psi_G|$  develops in Eq.18. Then the density order Eq.18 emerges as an independent order parameter. The SSDW crossovers to the stripe supersolid (SSS). One can write down a GL theory [28] in terms of the two independent order parameters  $\psi$  and  $\delta n$  and their mutual couplings. For example, the periodic potential  $\delta n = 2|\psi_G| \cos(k_0 x + \alpha)$  in Eq.18 acts as a periodic potential  $\delta n|\psi(x)|^2$  on the superfluid component  $\psi$ , so one can write down the generic expression for  $\psi$ :

$$\psi_{SSS} = \psi_0[1 + A|\psi_G| \cos(k_0 x + \alpha)] \quad (23)$$

where  $\psi_0 = \sqrt{a}e^{i(\vec{Q} \cdot \vec{x} + \phi)}$  and  $A$  is a numerical factor of the order 1. Well inside the stripe supersolid, the coupling between the two gapless modes  $\phi$  and  $\alpha$  leads to two branches of supersolidons [19].

As the boost increase further, the normal solid component  $|\psi_G|$  increases, the superfluid component  $\psi_{SSS}$  decreases and eventually disappears. There is a QPT from the SSS where  $\langle \psi_0 \rangle \neq 0, \langle \psi_G \rangle \neq 0$  to the stripe solid  $\langle \psi_0 \rangle = 0, \langle \psi_G \rangle \neq 0$  in Fig.2b. Just in terms of symmetry breaking, there is really no difference between the SSDW and the SSS, so Eq.21 where  $a \sim \rho_0$  and Eq.23  $a \ll \rho_0$  have the same symmetry breaking structure. But the former works best near the SF to the SSDW transition with  $z = 1$  where the SF component is non-critical, while the latter near the SSS to the stripe solid transition with  $z = 2$  where the SF component becomes critical.

So it resembles the extended boson Hubbard model [26, 27] where a stripe supersolid was shown to always exist slightly away from 1/2 filling both by microscopic calculations [21–25] and effective actions in the original basis [21–24] and the dual vortex basis [26, 27]. Due to the lack of C-symmetry, the vacancies usually have lower energies than that of interstitials, the stripe solid always host some vacancies. If their excitation energies  $E_v$  are positive, so can only be thermally excited. But when they become negative, they may undergo BEC. So approaching from the stripe solid side, the  $\psi_{SSS}$  in Eq.23 can be interpreted as the BEC of vacancies in the spontaneously formed stripe solid in Eq.18. The vacancies behave similarly as the holes on the top of the CDW or Valence Bond (VB) state at 1/2 filling examined in [26, 27] with  $z = 2$ . We expect it to be in the same class as the CDW to CDW-SS or VB to VB-SS transition [26, 27] with the dynamic exponent  $z = 2$ .

6. *Normal Liquid to stripe solid transitions.* In fact, by only keeping the  $\omega = 0$  component in Eq.20, it may also be used to describe the normal liquid to stripe solid transition at a finite  $T$  in Fig.2b. One need

only replace the superfluid density  $\rho_s$  by the normal liquid density  $\rho_n$ . The gap  $\Delta$  is the one in the density-density correlation function (the static structure factor)  $S(k) \sim \frac{1}{\Delta + \alpha(k^2 - k_0^2)^2}$  in the normal liquid. Then  $\tilde{r} > 0, \langle \psi_G \rangle = 0$ , it is in the normal liquid phase.  $\tilde{r} < 0, \langle \psi_G \rangle \neq 0$ , it is in the Stripe solid phase. Eq.22 still holds. The boost  $Q$  still plays an important role. It is in the 3d XY universality class which may also be understood as a stripe lattice melting transition driven by the phonons  $\alpha$  from the low temperature stripe solid side.

7. *Experimental realizations.* We study two kinds of instabilities: the one induced by the SF Goldstone mode near  $k = 0$  in the absence of rotons and the one induced by the roton mode near  $k = k_0$ . Here we discuss their experimental realizations respectively. The sound velocity in He4 is about  $v \sim 238m/s$ . In a conventional lab on the earth, taking a high way (magnetic levitated) train moving with a velocity  $300km/h \sim 83m/s$  is still below this characteristic velocity. A civil air-craft flight can reach even higher  $800km/h \sim 240m/s$  which just reaches the sound velocity in the Helium4. So the chance to see the instability near  $k = 0$  is unlikely on the earth. As mentioned in the introduction, in addition to the well known SF in the He4, there are also excitonic SF in the electronic systems in semi-conductors. The Bilayer Quantum Hall systems (BLQH) [4, 5] hosts the exciton SF in the charge neutral sector with the Goldstone mode velocity  $v_{BL} \sim 1.4 \times 10^4 m/s$ . The electron-hole bilayer system (EHBL) holds the exciton SF [6] with  $v_{EH} \sim 5 \times 10^3 m/s$ . It is essentially impossible except going to a satellite orbiting around the earth. In this regard, the weakly interacting cold atom BEC systems [2, 3] become better candidates with the SF Goldstone mode velocity  $v \sim 1cm/s$ .

The critical velocity due to the rotons in He4 is reduced to  $v \sim 60m/s$ , so Fig.2 can be mapped out by driving the SF beyond this critical velocity [17, 37]. Cold atom BEC systems with a long-range interaction such as a dipole-dipole interaction [38–41] or with spin-orbital couplings [44, 45] or dressed by Rydberg atoms [42, 43] also support rotons with much smaller critical velocities. So Fig.2 may find wide applications in these cold atom systems with tunable roton gaps.

8. *Conclusions.* Obviously, the SF and the stripe solid phase break two completely different symmetries: the former the internal  $U(1)_I$  symmetry whose breaking leading to the gapless Goldstone mode, the latter the translational symmetry whose breaking leading to the gapless lattice phonon modes. Just from general symmetry principle, there are two possibilities from the SF to the solid transition (1) a direct 1st order transition. This is the case driven by the pressure  $P$  in He4 in Fig.1a. The QPT near  $k = k_0$  is first order one driven by the pressure resulting a hcp solid structure, then the SF just disappears suddenly across the QPT. (2) It splits into two

second order ones with an intervening SS phase. This is the case in He4 driven by the boost or cold atom BEC with tunable rotons in Fig.2b. The QPT near  $k = k_0$  is second order one driven by the boost  $Q$  resulting a stripe solid structure, then the SF undergoes an accompanying second order QPT to a superfluid density wave (SDW). Then the Stripe SDW evolves into the stripe supersolid phase where the solid component is given by  $\delta\rho$ , the superfluid density wave component is given by its phase  $\psi_{SDW}$ . Finally the SSS phase gets into a stripe solid phase by kicking out of its SDW component  $\psi_{SDW}$  which stands for vacancies near the SSS to the stripe solid QPT. A microscopic calculation such as a QMC simulation is needed to test the existence of these vacancies and if they are stable against phase separations. If so, we may have discovered a new mechanism to realize a stable supersolid phase. Then the boost becomes an effective way to generate a supersolid which does not happen when increasing the pressure.

This work was originally initiated by the author's earlier works [19, 28] on putative SS in He4. I thank Moses Chan for helpful discussions during the very early stage of this work. I also thank Fadi Sun for the collaborations on two related works [8, 29].

---

[1] Anderson, Philip W. (1997) [1984]. Basic notions of condensed matter physics. Reading, Massachusetts: Addison-Wesley. ISBN 9780201328301.

[2] K. B. Davis, M. -O. Mewes, M. R. Andrews, N. J. van Druten, D. S. Durfee, D. M. Kurn, and W. Ketterle, Bose-Einstein Condensation in a Gas of Sodium Atoms, *Phys. Rev. Lett.* 75, 3969 (1995) - Published 27 November 1995

[3] M. W. Zwierlein, C. A. Stan, C. H. Schunck, S. M. F. Raupach, A. J. Kerman, and W. Ketterle, Condensation of Pairs of Fermionic Atoms near a Feshbach Resonance, *Phys. Rev. Lett.* 92, 120403 (2004) - Published 25 March 2004

[4] For reviews of bilayer quantum Hall systems, see S. M. Girvin and A. H. Macdonald, in *Perspectives in Quantum Hall Effects*, edited by S. Das Sarma and Aron Pinczuk ( Wiley, New York, 1997).

[5] Longhua Jiang and Jinwu Ye, Ground state, quasihole and a pair of quasihole wavefunctions in Bi-layer Quantum Hall systems, *Phys. Rev. B* 74, 245311 (2006).

[6] Jinwu Ye, T. Shi and Longhua Jiang, Angle resolved Photoluminescence spectrum from exciton condensate in electron-hole semiconductor bilayers, *Phys. Rev. Lett.* 103, 177401 (2009).

[7] Subir Sachdev, T. Senthil, and R. Shankar, Finite-temperature properties of quantum antiferromagnets in a uniform magnetic field in one and two dimensions, *Phys. Rev. B* **50**, 258 (1994).

[8] Fadi Sun and Jinwu Ye, Response of a strongly interacting spin-orbit coupling system to a Zeeman field long version arXiv:2011.11287, version 2.

[9] Jongchul Mun, Patrick Medley, Gretchen K. Campbell, Luis G. Marcassa, David E. Pritchard, and Wolfgang Ketterle, Phase Diagram for a Bose-Einstein Condensate Moving in an Optical Lattice, *Phys. Rev. Lett.* 99, 150604 (2007) - Published 12 October 2007

[10] L. D. Landau, *J. Phys. USSR* 5, 71 (1941)

[11] R. P. Feynman, "Progress in Low- Temperature Physics", *loc. cit*

[12] J. S. Langer and Michael E. Fisher, Intrinsic Critical Velocity of a Superfluid, *Phys. Rev. Lett.* 19, 560 Published 4 September 1967

[13] For a review, see A.L. Fetter and J. D. Walecka, *Quantum Theory of many-particle Systems*, Dover Publications, Inc. Mineola, New York, 2002.

[14] G. E. Astrakharchik and L. P. Pitaevskii, Motion of a heavy impurity through a Bose-Einstein condensate, *Phys. Rev. A* 70, 013608 (2004) - Published 20 July 2004

[15] Gordon Baym and C. J. Pethick, Landau critical velocity in weakly interacting Bose gases, *Phys. Rev. A* 86, 023602 Published 2 August 2012

[16] A. Andreev and I. Lifshitz, *Sov. Phys. JETP* 29, 1107 (1969); G. V. Chester, *Phys. Rev. A* 2, 256 (1970); A. J. Leggett, *Phys. Rev. Lett.* 25, 1543 (1970); W. M. Saslow , *Phys. Rev. Lett.* 36, 1151?1154 (1976).

[17] E. Kim and M. H. W. Chan, *Nature* 427, 225 - 227 (15 Jan 2004), E. Kim and M. H. W. Chan, *Science* 24 September 2004; 305: 1941-1944,

[18] For a collection of theoretical and experimental works inspired by Chan's experimental results, see a special issue in *Journal of Low Temperature Physics*, 2012, edited by..... It also includes the author's [19].

[19] Yu Chen, Jinwu Ye and Quang Shan Tian, Classification of a supersolid: Symmetry breaking and Excitation spectra, *Journal of Low Temperature Physics*: 169 (2012), 149-168.

[20] Duk Y. Kim and Moses H. W. Chan, Absence of Supersolidity in Solid Helium in Porous Vycor Glass, *Phys. Rev. Lett.* 109, 155301 Published 8 October 2012.

[21] G. Murthy, D. Arovas, and A. Auerbach, *Phys. Rev. B* **55**, 3104 (1997).

[22] R. G. Melko, et al, *Phys. Rev. Lett.* **95**, 127207 (2005).

[23] D. Heidarian and K. Damle, *Phys. Rev. Lett.* **95**, 127206 (2005);

[24] S. Wessel and M. Troyer, *Phys. Rev. Lett.* **95**, 127205 (2005).

[25] Jing Yu Gan, Yu Chuan Wen, Jinwu Ye, Tao Li, Shi-Jie Yang, Yue Yu, *Phys. Rev. B* **75**, 214509 (2007).

[26] Ye, J. Duality, magnetic space group and their applications to quantum phases and phase transitions on bipartite lattices in several experimental systems. *Nucl. Phys. B* **805**, 418 (2008). here, we also find a new kind of supersolid called valenced bond supersolid.

[27] Jinwu Ye and Chen Yan, Quantum phases, Supersolids and quantum phase transitions of interacting bosons in frustrated lattices, *Nucl. Phys. B* 869 (2013), 242-281

[28] Jinwu Ye, Elementary excitations, Spectral weights and Experimental signatures of a Supersolid and Larkin-Ovchinnikov-Fulde - Ferrell (LOFF) state, *J. Low Temp Phys.* 160(3), 71-111,(2010)

[29] Fadi Sun and Jinwu Ye, Quantum Phase transitions observed in a moving frame and emergent space-time near Quantum Phase transitions.

[30] Fisher M. P. A., Weichman P. B., Grinstein G. and Fisher D. S., *Phys. Rev. B* 40, 546 (1989).

[31] For example, in the C-symmetry case, the phase and

magnitude in Eq.1 are not conjugate variables anymore. In fact, they become independent, the magnitude mode becomes an independent Higgs mode. See [8, 29] for details.

[32] Fadi Sun, Jinwu Ye, Wu-Ming Liu, Fermionic Hubbard model with Rashba or Dresselhaus spinorbit coupling, *New J. Phys.* 19, 063025 (2017).

[33] Here, we only use the mean field ground state for the SF or BSF. In fact, as shown in [5] in the context of exciton SF in BLQH and [32] in the context of a Y-y magnetic state in a fermionic SOC system, the mean field ground state will be modified by the quantum fluctuations in the ground state which is determined by the excitation spectrum even at  $T = 0$ .

[34] Longhua Jiang and Jinwu Ye, Lattice structures of Larkin-Ovchinnikov-Fulde - Ferrell (LOFF) state, *Phys. Rev. B* 76, 184104 (2007).

[35] It maybe constructive to compare the lattice phonon mode here with that in a lattice mode represented in [8], here  $a$  in  $x \rightarrow x + a$  is any real number, the  $k_0$  is also any real number, then  $\theta = k_0 a$  is a continuous number, it comes from a continuous translation symmetry breaking to a lattice translation normal to the stripe resulting the lattice phonon mode. While in the lattice  $x \rightarrow x + a$  where  $a$  must be a lattice constant,  $k_0 a$  is a continuous number only when  $k_0$  is an In-commensurate number. it comes from the discrete lattice translation symmetry  $x \rightarrow x + a$  breaking to none resulting the gapless phason mode.

[36] Here, we use the 2 + 1 d notation. Due to the rotation symmetry in the  $YZ$  plane, one may just set  $q_y^2 \rightarrow q_y^2 + q_z^2$  in the 3d He4 case.

[37] Jacques Bossy, Jonathan V. Pearce, Helmut Schober, and Henry R. Glyde, Phonon-Roton Modes and Localized Bose-Einstein Condensation in Liquid Helium under Pressure in Nanoporous Media, *Phys. Rev. Lett.* 101, 025301 (2008) - Published 11 July 2008

[38] P. B. Blakie, D. Baillie, and R. N. Bisset, Roton spectroscopy in a harmonically trapped dipolar Bose-Einstein condensate, *Phys. Rev. A* 86, 021604(R) (2012) - Published 15 August 2012

[39] D. Petter, G. Natale, R.M.W. van Bijnen, A. Patscheider, M.J. Mark, L. Chomaz, and F. Ferlaino, Probing the Roton Excitation Spectrum of a Stable Dipolar Bose Gas, *Phys. Rev. Lett.* 122, 183401 (2019) - Published 8 May 2019

[40] John P. Corson, Ryan M. Wilson, and John L. Bohn, Stability spectroscopy of rotons in a dipolar Bose gas, *Phys. Rev. A* 87, 051605(R) (2013) - Published 21 May 2013

[41] R. N. Bisset, D. Baillie, and P. B. Blakie, Roton excitations in a trapped dipolar Bose-Einstein condensate, *Phys. Rev. A* 88, 043606 (2013) - Published 7 October 2013

[42] Gary McCormack, Rejish Nath, and Weibin Li, Dynamical excitation of maxon and roton modes in a Rydberg-dressed Bose-Einstein condensate, *Phys. Rev. A* 102, 023319 (2020) - Published 19 August 2020

[43] N. Henkel, R. Nath, and T. Pohl, Three-Dimensional Roton Excitations and Supersolid Formation in Rydberg-Excited Bose-Einstein Condensates, *Phys. Rev. Lett.* 104, 195302 (2010) - Published 11 May 2010

[44] Si-Cong Ji, Long Zhang, Xiao-Tian Xu, Zhan Wu, Youjin Deng, Shuai Chen, and Jian-Wei Pan, Softening of Roton and Phonon Modes in a Bose-Einstein Condensate with Spin-Orbit Coupling, *Phys. Rev. Lett.* 114, 105301 (2015) - Published 9 March 2015

[45] Hao Lyu, Yongping Zhang, and Thomas Busch, Detection of roton and phonon excitations in a spin-orbit-coupled Bose-Einstein condensate with a moving barrier, *Phys. Rev. A* 106, 013302 (2022) - Published 5 July 2022